Studies of the Crystalline–Liquid Crystalline Phase Transition of Lipid Model Membranes. III. Structure of a Steroid–Lecithin System below and above the Lipid-Phase Transition

H. Träuble* and E. Sackmann

Contribution from the Max-Planck-Institut für Biophysikalische Chemie, 34 Göttingen, Nikolausberg, Germany. *Received August 27, 1971*

Abstract: Theoretical models for the organization of mixed steroid–lecithin membranes are developed and checked against electron spin resonance measurements. In part II of this series we had determined values of the exchange interaction W_{ex} between androstane spin labels within dipalmitoyllecithin model membranes by computer analysis of esr spectra. Comparison of such data with theoretical considerations permits one to determine the molecular organization of mixed membranes. A good criterion for the validity of theoretical models is provided by comparison with the measured dependence of W_{ex} on the molar ratio steroid:lecithin, c, and the temperature. The most important result is the observation that the organization of androstane–lecithin membranes depends critically upon the crystalline–liquid crystalline phase transition of the lecithin. Different functional dependencies of W_{ex} on the steroid concentration (c) are observed at temperatures below and above the transition point (T_t). Above T_t the steroid and lecithin molecules form an ideal mixture. The steroid molecules, and most probably also the lipid molecules, undergo translational diffusion within the plane of the membrane. The diffusion coefficient is determined as $D_{diff} = 10^{-8}$ cm^2/sec, corresponding to an average travel distance of about 10,000 Å in 1 sec. Below the phase transition the lipid matrix is less fluid. Substantial translational diffusion within the plane of the membrane is not possible. Also the tumbling motion of the molecules is less rapid ($\nu \approx 10^8$ Hz). Below T_t the organization of the mixed system can be described as a mosaic structure with very small steroid clusters embedded within the lipid matrix. The concentration of the clusters, their size and shape, and the number of steroid molecules per cluster can be determined from the experimental data. The density n of clusters is independent of the molar ratio steroid:lipid (c). For $T = 19°$, $n = 3.36 \times 10^{11}$/cm^2. The clusters increase with increasing steroid concentration. For $c = 0.035$ the cluster radius is $r = 30$ Å, the average distance between the clusters is 285 Å, and about 65 steroid molecules are assembled per cluster. The thermal transition between the two organization forms is reversible. Upon heating the system above the phase transition the clusters dissolve and a homogeneous mixture is formed. The phase transition produces an expansion of the lipid lattice. The value of this expansion and the temperature dependence of the lattice constant, a, can be determined from the temperature dependence of the esr spectra. The possible importance of our results for the structure and function of biological membranes is discussed.

1. Introduction

In two previous papers[1,2] (cited as part I and II in the following) we reported optical and electron spin resonance measurements of the crystalline–liquid crystalline phase transition of mixed steroid–lecithin model membranes. These experiments were performed with aqueous dispersions which contained as a lipid component synthetic dipalmitoyllecithin with a characteristic transition temperature T_t of about 41°. The steroid component which served as a spin label was an androstane derivative with a paramagnetic N–O group (*cf.* Figure 1). These experiments were performed in an attempt (1) to learn more about the structural changes of the lipid matrix at the phase transition and (2) to investigate the influence of the phase transition on the organization of mixed steroid–lecithin model membranes. As is known from studies by Chapman and coworkers,[3–7] the lipid phase transition causes a "fluidization" or an increase in mobility of the hydrocarbon chains of the lipid molecules. Thus it was expected that the phase transition affects also the organization of mixed steroid–lecithin systems.

The optical measurements were performed with fluorescent and absorbing probes (8-anilino-1-naphthalene sulfonate, Bromthymol Blue) which bind to the membrane surface and indicate changes in the arrangement of the lipid polar head groups at the phase transition.[8] These measurements have shown that the phase transition is accompanied by changes in the polar group arrangement.

The spin-labeling technique was used to detect conformational changes within the hydrocarbon phase of the membranes at the phase transition. As is well known[9] the esr spectra depend very sensitively upon the mobility, the mutual orientation, and the arrangement of the spin labels within the lipid matrix. The measurements described in part I show that the shape of the esr spectra varies with the concentration c of the steroid molecules (c = molar ratio label:lipid). These spectral changes are due to magnetic interactions (dipole–dipole and spin-exchange interaction) between the spin labels and thus reflect the arrangement of the steroid molecules within the lipid matrix. Therefore an analysis of the esr line shape (*cf.* part II) yields information about the organization of the mixed membranes. In part II we have determined the exchange

(1) E. Sackmann and H. Träuble, *J. Amer. Chem. Soc.*, **94**, 4482 (1972).
(2) E. Sackmann and H. Träuble, *J. Amer. Chem. Soc.*, 94, 4492 (1972).
(3) D. Chapman, "The Structure of Lipids," Methuen, London, 1965.
(4) B. D. Ladbrooke and D. Chapman, *Chem. Phys. Lipids*, **3**, 304 (1969).
(5) D. Chapman, R. M. Williams, and B. D. Ladbrooke, *ibid.*, 1, 445 (1967).
(6) D. Chapman, D. Byrne, and G. G. Shipley, *Proc. Roy. Soc., Ser. A*, **290**, 115 (1966).
(7) M. S. Phillips, R. M. Williams, and D. Chapman, *Chem. Phys. Lipids*, **3**, 234 (1969).
(8) H. Träuble, *Naturwissenschaften*, **58**, 277 (1971).
(9) H. M. McConnell and B. G. McFarland, *Quart. Rev. Biophys.*, **3**, 91 (1970).

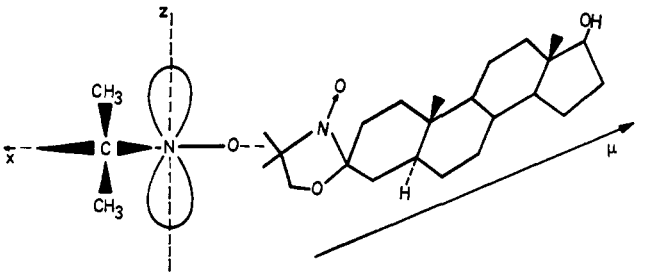

Figure 1. Chemical structure of the *N*-oxyl-4′,4′-dimethyloxazolidine derivative of 5α-androstan-3-one-17β-ol, which was used as a spin labeled steroid. The unpaired electron is located at the nitrogen atom of the N–O group in a 2pπ orbital. The more hydrophilic end of the molecule is determined by the OH group. Left hand side: definition of the principal axes system of the hyperfine coupling tensor T, assuming planarity of the oxazolidine ring. The long axis of the 2pπ orbital is perpendicular to the long axis of the steroid molecule.

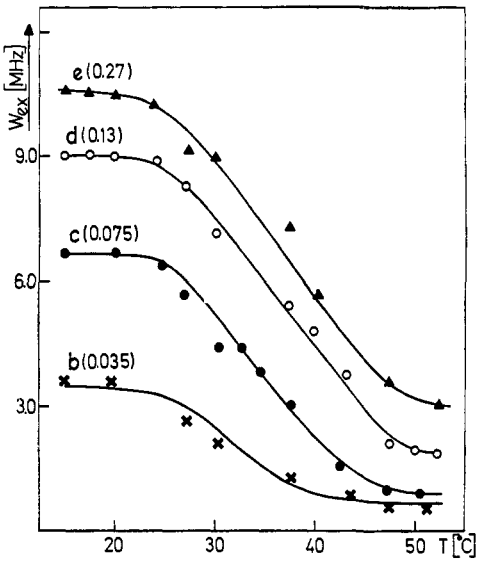

Figure 2. Temperature dependence of the exchange frequency W_{ex} calculated by computer simulation of the experimental spectra presented in Figure 7, part I. In the computer calculation both the exchange interaction and the dipolar interaction between the radicals were taken into account. Notations: letter = number of preparation; in brackets, molar ratio label:lipid.

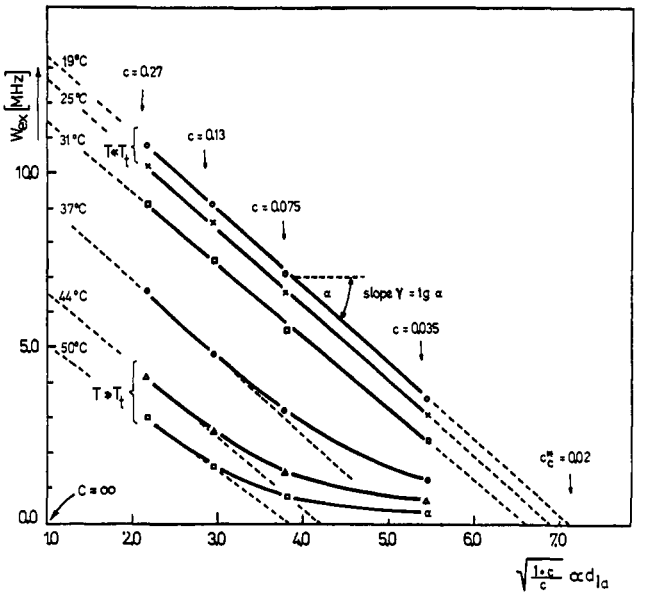

Figure 3. Concentration dependence of the exchange frequency W_{ex} at different temperatures. W_{ex} is plotted against $\sqrt{(1+c)/c}$; this expression is proportional to the average distance d_{la} between the steroid molecules within the lipid matrix (*cf.* eq 5). c denotes the molar ratio label:lipid. Straight lines are obtained for $T \ll T_t$ where T_t denotes the temperature of the lipid-phase transition. For $T \gg T_t$ the curves do not extrapolate to zero for finite concentrations. The intercepts of the straight lines with the abscissa define critical concentrations c_c^* suggesting $W_{ex} = 0$ for $c < c_c^*$; the intercepts with the ordinate at $c = \infty$ define maximal values $\hat{W}_{ex}$ (see text).

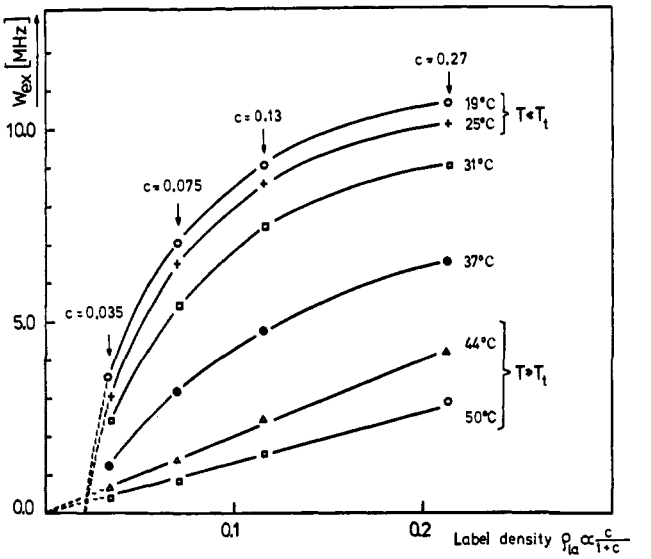

Figure 4. Concentration dependence of W_{ex} for different temperatures. W_{ex} is plotted against the label density $\rho_{la} \propto c/(1+c)$. For $T \gg T_t$ straight lines are obtained extrapolating through the origin. For $T \ll T_t$ the measured points yield parabolic curves which cut the abscissa at critical values c_c^* ($W_{ex} = 0$ for $c < c_c^*$).

frequency W_{ex} from the esr spectra. This parameter depends sensitively upon the precise structure of the mixed system: (a) a sharp decrease in W_{ex} occurs in the temperature range of the crystalline–liquid crystalline phase transition; (b) the concentration dependence of W_{ex} is different above and below the phase transition. It was suggested in part II that these effects indicate a change in the organization of the steroid-in-lecithin system at the phase transition. It is the aim of the present paper to develop theoretical models for the structure of the mixed steroid–lecithin system on the basis of the data presented in parts I and II.

2. Summary of the Esr Measurements

In part I esr spectra were recorded at different steroid concentrations ranging from $c = 0.01$ to $c = 0.27$ in the temperature range between 18 and 55° which covers the region of the lipid-phase transition. For low label concentration, *i.e.*, in the absence of interactions between the label molecules, clearly resolved triplet spectra are observed. For $T < T_t$ increasing label concentration produces broadened esr spectra (*cf.* Figure 7, part I). Upon heating the system above T_t these broad spectra resolve into sharp triplet spectra. In part II these spectra were analyzed in terms of the magnetic dipole–dipole interaction and the spin-exchange inter-

action between the nitroxide radicals. The following theoretical considerations will be based on the experimental results for the temperature and concentration dependence of the spin-exchange frequency W_{ex}. These functional dependencies of W_{ex} as determined in part II are shown in Figures 2–4.

(a) Temperature Dependence of W_{ex} (Figure 2). For all label concentrations W_{ex} decreases sharply with increasing temperature between about 30 and 40°, *i.e.*, in the temperature range of the lipid-phase transition. The values of W_{ex} at $T = 20°$ and $T = 52°$ are summarized in Table I. According to this table the relative decrease of W_{ex} is roughly the same for all concentrations and can be written as

$$\frac{W_{ex}(20°) - W_{ex}(50°)}{W_{ex}(20°)} = \frac{\Delta W_{ex}}{W_{ex}(20°)} \approx 0.80 \quad (1)$$

This equation states that upon heating the system above the phase transition the exchange interaction is reduced by about 80%.

Table I. Values of the Exchange Frequency W_{ex} at $T = 20°$ and $T = 52°$ for Different Label:Lipid Molar Ratios c[a]

Prepn No.	c[b]	W_{ex}, MHz 20°, $T \ll T_t$	W_{ex}, MHz 52°, $T \gg T_t$	ΔW_{ex}[c]	$\Delta W_{ex}/W_{ex}(20°)$
b	0.035	3.5	0.6	2.9	0.83
c	0.075	6.7	0.9	5.8	0.85
d	0.13	9.0	1.8	7.2	0.80
e	0.27	10.5	3.0	7.6	0.72

[a] *Cf.* Figure 2. The relative decrease in W_{ex} in the region of the phase transition is nearly the same for all label concentrations. [b] Equals the molar ratio label:lipid. [c] Equals $W_{ex}(20°) - W_{ex}(52°)$.

(b) Concentration Dependence of W_{ex}. The concentration dependence of W_{ex} is shown in Figures 3 and 4 for temperatures between 19 and 50°. In Figure 3 the W_{ex} values are plotted against $\sqrt{(1 + c)/c}$; this expression is proportional to the average next-nearest-neighbor distance d_{1a} between the label molecules, assuming statistical distribution within the lipid matrix. In Figure 4 the W_{ex} values are plotted against the density ρ_{1a} (per cm²) of the label molecules. Obviously different functional dependencies between W_{ex} and c are valid below and above the phase transition.

The average label distance d_{1a} and the label density ρ_{1a} can be calculated from the molar ratio c label:lipid in the following way. Defining ρ as the total number of molecules (lipid + label) per square centimeter, $\rho = 1/F$, where F = molecular area. As an approximation F is assumed to be equal for steroid and lipid molecules. ρ_{1a} = number of label molecules per cm²; ρ_{1i} = number of lipid molecules per cm². Then $\rho = \rho_{1a} + \rho_{1i}$, and the molar ratio label:lipid

$$c = \rho_{1a}/\rho_{1i} \quad (2)$$

This leads to

$$\rho_{1a} = \rho \cdot \frac{c}{1 + c} = \frac{1}{F} \cdot \frac{c}{(1 + c)} \quad (3)$$

Assuming that the label molecules form a triangular lattice with a lattice constant d_{1a} we obtain

$$\rho_{1a} = 2/d_{1a}^2\sqrt{3} \quad (4)$$

Combining eq 3 and 4 yields

$$d_{1a} = \sqrt{\frac{2F}{\sqrt{3}}}\sqrt{\frac{1 + c}{c}} \quad (5)$$

The functional dependencies between W_{ex} and c for $T \ll T_t$ and $T \gg T_t$ can be read from Figures 3 and 4.

$T \ll T_t$. From Figure 3 the following relation is found

$$W_{ex} = \hat{W}_{ex} - \gamma\{\sqrt{(1 + c)/c} - 1\} \quad (6)$$

where $\hat{W}_{ex}$ is the intercept of the curves in Figure 3 with the ordinate at $c \to \infty$. This value represents the maximum possible exchange frequency for a given temperature. $\hat{W}_{ex}$ can be interpreted as the exchange frequency of a system of closely packed label molecules. It will be assumed later that the closest packing of the label molecules in the mixed steroid-in-lecithin system is determined by the packing of the supporting lipid matrix.

For $T = 19°$ eq 6 reads

$$W_{ex}[\text{MHz}] = 13.4 - 2.20\{\sqrt{(1 + c)/c} - 1\} \quad (7)$$

The intercepts of the straight lines in Figure 3 with the abscissa determine lower critical values c_c^* (*cf.* Table II) which are characterized by $W_{ex} = 0$ when $c < c_c^*$ or $d > d_c^*$.

Table II. Parameters Describing the (Asymptotic) Straight Lines (---) in Figure 3[a]

	T, °C	$\hat{W}_{ex}$, MHz	γ[b]	$\sqrt{(1 + c_c^*)/c_c^*}$ at $W_{ex} = 0$	c_c^*[c]	d_c^*, Å[d]
$T < T_t$	19	13.4	2.20	7.1	0.0202	52.0
	25	12.54	2.16	6.9	0.0215	51.4
	31	11.5	2.09	6.5	0.0242	48.5
$T > T_t$	37	9.0	2.22	5.1	0.0400	42.0
	44	6.7	2.17	4.1	0.0634	33.6
	50	5.0	2.20	3.8	0.0745	28.7

[a] Algebraic description of these lines: $W_{ex} = \hat{W}_{ex} - \gamma\{\sqrt{(1 + c)/c} - 1\}$. $\hat{W}_{ex}$ = maximum exchange frequency determined by the intercepts of the straight lines in Figure 3 with the ordinate at $c = \infty$. c_c^* = critical values of the molar ratio label:lipid, calculated from the intercepts of the asymptotic lines in Figure 3 with the abscissa. The corresponding next-nearest-neighbor distances d_c^* were calculated from eq 5 using $F = 48$ Å² for $T < T_t$ and $F = 58$ Å for $T > T_t$. [b] Equals the slope of the straight lines in Figure 3. [c] The critical molar ratio label:lipid. [d] The critical label distance.

$T \gg T_t$. From Figure 4 a linear dependence between W_{ex} and $c/(1 + c)$ is found. For $T = 50°$

$$W_{ex}[\text{MHz}] = 13.5c/(1 + c) \quad (8)$$

3. Models

Introductory Remarks. The exchange frequency W_{ex} between two immobilized radicals is proportional to the exchange integral J (*cf.* eq 6, part II). Therefore W_{ex} decreases rapidly with increasing distance d between the radicals. Approximating the $2p\pi$ orbitals of the unpaired electrons of the nitroxide radicals by Slater orbitals, J is found to decrease exponentially with increasing distance d between the radicals[10]

$$W_{ex} = A \cdot e^{-\alpha d} \quad (9)$$

(10) R. Stuart and W. Marshall, *Phys. Rev.*, 120, 353 (1960).

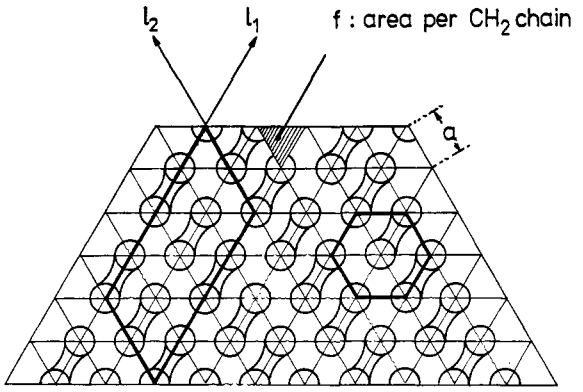

Figure 5. Triangular lattice formed by closely packed hydrocarbon chains of lipid molecules.[12] The lattice of the lipid molecules is anisotropic and exhibits two preferred directions of packing l_1 and l_2.

A and α are constants which can be determined experimentally. J can be approximated by setting J = constant ($\neq 0$) for $d \leqslant d_c$ and $J = 0$ for $d > d_c$, corresponding to W_{ex} = constant ($\neq 0$) for $d \leqslant d_c$ and $W_{ex} = 0$ for $d > d_c$.

The critical distance d_c may be defined as follows. (a) Two interacting radicals

$$0.95\int_{d_o}^{\infty} W_{ex}\,dr = \int_{d_o}^{d_c} W_{ex}\,dr$$

Here d_o denotes a lower cut-off distance given by the distance of closest approach of the two interacting radicals. Integration leads to

$$d_c = d_o + \ln 20/\alpha \tag{10}$$

(b) Two-dimensional statistical distribution of radicals with radical density ρ

$$0.95\int_{d_o}^{\infty} 2\pi r\rho W_{ex}\,dr = \int_{d_o}^{d_c} 2\pi r\rho W_{ex}\,dr$$

Integrating and approximating $d_o\alpha \ll 1$ leads to

$$d_c = \frac{1}{\alpha}(2 - 0.1B)^{1/2} \tag{11a}$$

where

$$B = (1 + \alpha d_o)e^{-\alpha d_o} \tag{11b}$$

3.1. Static Model. In this model it is assumed that the label molecules are distributed statistically within the lipid matrix and cannot perform translational diffusion. In order to explain the observed decrease of W_{ex} with increasing temperature it must be assumed that the average distance between the label molecules increases with increasing temperature at T_t. This is equivalent to the assumption of a lateral expansion of the membrane at the phase transition. There is, indeed, strong evidence for a lateral expansion of the lipid matrix at T_t. This evidence is provided by X-ray diffraction studies[5] and by dilatometric measurements[11] with lamellar dipalmitoyllecithin–water systems.

For $T \ll T_t$ the X-ray studies yield a value of 46 Å for the bilayer thickness and a value of $F = 48$ Å^2 for the molecular area. A value of 4.19 Å is obtained for the shortest spacing. The sharpness of the X-ray pattern for $T \ll T_t$ indicates that the lipid molecules are packed in a regular two-dimensional lattice; most probably the hydrocarbon chains form a triangular lattice[12] (*cf.* Figure 5). Upon heating the system above T_t the short spacing (4.19 Å) goes over into a diffuse line (4.6 Å) and the bilayer thickness decreases sharply by about 5 Å. This decrease is attributed to a shortening of the hydrocarbon chains.[5] Dilatometric measurements[11] on this same system yield a small volume increase of $\Delta V/V \approx 1.5\%$ at the phase transition.

Combination of the X-ray data and the dilatometric measurements leads to the conclusion that at the phase transition the molecular area F increases from F = 48 Å^2 ($T \ll T_t$) to F = 58 Å^2 ($T \gg T_t$) corresponding to a relative increase of the molecular area F by about 17–20%.

For a triangular lattice of the hydrocarbon chains as depicted in Figure 5, the area f per CH_2 chain and the lattice constant a are related through

$$f = a^2\sqrt{3}/2 \tag{12}$$

Thus the area F per lipid molecule is

$$F = a^2\sqrt{3} \tag{13}$$

This leads to

$$da/a = {}^1/_2 dF/F \tag{14}$$

Thus the observed change in molecular area $dF/F \approx 20\%$ at the phase transition is equivalent to $da/a \approx 10\%$.

The corresponding change in W_{ex} can be estimated as follows. The measured exchange frequency W_{ex} per radical is a result of exchange interactions with all neighboring radicals. Denoting the label density by ρ_{la}, W_{ex} is expressed as

$$W_{ex}(d) = \int_{d_o}^{d} \rho_{la} 2\pi r W_{ex}'\,dr$$

with

$$W_{ex}' = A \cdot e^{-\alpha r}$$

Integration yields

$$W_{ex}(d) = (2\pi A\rho_{la}/\alpha^2)\{B - (1 + \alpha d)e^{-\alpha d}\} \tag{15a}$$

where B is given by eq 11b.

For $d \rightarrow \infty$ we obtain

$$W_{ex} = (2\pi A\rho_{la}/\alpha^2)B \tag{15b}$$

Using eq 3 yields

$$W_{ex} = \frac{2\pi AB}{\alpha^2}\cdot\frac{1}{F}\cdot\frac{c}{(1+c)} \tag{16}$$

Equation 16 leads to

$$\Delta W_{ex}/W_{ex} = -\Delta F/F \tag{17}$$

The maximum value of the exchange frequency, $\hat{W}_{ex}$, is obtained for $c \rightarrow \infty$

$$\hat{W}_{ex} = 2AB/\alpha^2 F \tag{18}$$

Equations 15 and 16 are valid only for $c > c_c$ or $d < d_c$. This is due to the fact that $W_{ex} = 0$ for $d > d_c$ ($c < c_c$) or $\rho_{la} < \rho_{la,c}$ and that the label molecules were assumed to be immobile with respect to translational diffusion.

(11) H. Träuble and D. Haynes, *J. Chem. Phys. Lipids*, 7, 324 (1971).

(12) B. A. Pethica, *Soc. Chem. Ind. London, Monogr.*, 19, 85 (1965).

The present model predicts (1) a linear dependence between $\Delta W_{ex}/W_{ex}$ and $\Delta F/F$ according to eq 17, and (2) a linear increase of W_{ex} with $c/(1+c)$ for $c > c_c$ and $W_{ex} = 0$ for $c < c_c$.

The observed change in $\Delta W_{ex}/W_{ex}$ has the right sign but is by a factor of 4 larger ($\Delta W_{ex}/W_{ex} = 0.80$) than the value expected from the change in molecular area ($\Delta F/F \approx 0.17$–0.20). Concerning the second point, the experimental results for $T \ll T_t$ [$W_{ex} \propto \sqrt{(1+c)/c}$] are in clear contradiction to the expectation. For $T \gg T_t$ the exchange frequency increases linearly with $c/(1+c)$, as expected, but there exists no lower limit c_c for which $W_{ex} = 0$ when $c < c_c$.

In summarizing it may be said that the static model is certainly not true for $T \ll T_t$ and that most probably it is not applicable for $T \gg T_t$.

3.2. Diffusional Model. The spin exchange has been studied by several authors as a function of temperature T, viscosity η, and pressure p for liquid solutions of paramagnetic radicals.[13–17] The spin exchange was found to be roughly linear in T/η.[17] This result may be understood on the basis of a diffusional model proposed by Pake and Tuttle.[14] In this model the exchange frequency is written as

$$W_{ex} = \nu_{enc} \cdot p \tag{19}$$

where ν_{enc} denotes the frequency of encounters between the radicals and p is the probability of exchange upon each encounter ($0 \leqslant p \leqslant 1$). The time between two encounters $\tau_{enc} = 1/\nu_{enc}$ is assumed to be large compared to the encounter time t_{enc}. An effective interaction distance d_c is defined assuming W_{ex} = constant for $d \leqslant d_c$ and $W_{ex} = 0$ for $d > d_c$.

The frequency of encounters ν_{enc} can be estimated on the basis of a diffusional model. For the two-dimensional system given in our case, ν_{enc} is the product of the area which the radical sweeps per second, multiplied by the density ρ_{1a} of radicals. Thus

$$\nu_{enc} = 2d_c \cdot l \cdot \rho_{1a} = 2d_c \cdot l \cdot \frac{1}{F} \cdot \frac{c}{(1+c)} \tag{20}$$

where l denotes the integrated distance of travel per second, and d_c is the effective interaction diameter of the radicals.

The exact mechanism of diffusion of the steroid molecules within the lipid matrix is not known; it could be a vacancy, interstitial, or interchange mechanism. However, in all cases the diffusion coefficient can be written as

$$D_{diff} = \theta \cdot \nu \cdot \lambda^2 \tag{21}$$

where ν is the hopping frequency ($\nu = \nu_0 \cdot e^{-\Delta G/kT}$), λ is the length of one jump, determined by the lattice constant, and θ is a geometrical factor, which can be taken equal to $1/2$. Writing $l = \nu\lambda = D_{diff}/\theta\lambda$ yields

$$\nu_{enc} = 2d_c \frac{c}{(1+c)} \frac{1}{F} \frac{D_{diff}}{\theta\lambda} \tag{22}$$

or

$$W_{ex} = 2d_c \frac{c}{(1+c)} \frac{1}{F} \frac{D_{diff}}{\theta\lambda} p \tag{23}$$

The diffusional model thus leads to the same concentration dependence as the static model ($W_{ex} \propto c/(1+c)$; however, there is no critical concentration c_c for which $W_{ex} = 0$ when $c < c_c$. The reason for this is that in a diffusional model there is always a certain probability ($\neq 0$) for radical encounters.

The experimental results for $T \gg T_t$ are in accord with the predictions of the diffusional model. Identifying expression 23 with the experimental result (eq 8) and taking $p = 1$ (*cf.* below) leads to

$$2d_c D_{diff}/F\theta\lambda = 13.5 \times 10^6$$

Taking $F = 58$ Å^2, $\lambda = 8$ Å, $\theta = 1/2$, and $d_c = 20$ Å (*cf.* below) yields for the translational diffusion coefficient of the steroid molecules within the lipid matrix the value[18]

$$D_{diff} \approx 1 \times 10^{-8} \text{ cm}^2/\text{sec}$$

This value is about a thousand times smaller than the typical values for the diffusional coefficient in liquids. From D_{diff} we estimate a hopping frequency $\nu \approx 3 \times 10^6$/sec.

In the diffusional model the temperature dependence of W_{ex} is determined chiefly by the temperature dependence of D_{diff} and by a possible temperature dependence of the exchange probability p. In the general case p must be considered as a function of the exchange integral J and the time of encounter t_{enc} ($\propto d_c/\nu\lambda$) and thereby as a function of the temperature. However, for $Jt_{enc} \gg 1$, $p \approx 1$.

The value of p may be judged from studies of the spin exchange in liquids. For liquids D_{diff} can be expressed by the Stokes–Einstein relation, which leads to

$$W_{ex} \propto (T/\eta) \cdot p$$

where η is the solvent viscosity.

Experimental studies of the spin exchange in solution of di-*tert*-butyl nitroxide in *n*-pentane and propane and other systems[15–17] yield as a general result that W_{ex} is roughly linear in T/η indicating that the exchange probability is constant with respect to T/η. This suggests $Jt_{enc} \gg 1$ and $p \approx 1$ for liquid solutions. In our case the diffusing molecules are rather large and the diffusion medium has a quasicrystalline structure. Thus t_{enc} is certainly larger than in liquids and therefore $p = 1$.

The temperature dependence of W_{ex} is therefore determined by the temperature dependence of the diffusion coefficient D_{diff} (*cf.* eq 23) and W_{ex} is expected to increase exponentially with increasing temperature. In contrast to this the measurements yield a sharp decrease of W_{ex} with increasing temperature in the range of the lipid-phase transition (*cf.* Figure 2). This result is very surprising because the lipid-phase transition produces an increase in the fluidity of the hy-

(13) K. H. Hausser, *Z. Naturforsch. A*, **14**, 425 (1959).
(14) G. E. Pake and T. R. Tuttle, *Phys. Rev. Lett.*, **3**, 423 (1959).
(15) J. G. Powles and M. H. Mosley, *Proc. Phys. Soc.*, **78**, 37d (1961).
(16) N. Edelstein, A. Kwok, and A. H. Maki, *J. Chem. Phys.*, **41**, 3473 (1964).
(17) W. Plachy and D. Kivelson, *ibid.*, **47**, 3312 (1967).

(18) We are very grateful to Dr. McConnell for pointing out that our derivation most probably underestimates the value of D_{diff}. This is due to the fact that only collisions between molecules with different electron and nuclear spin states lead to exchange broadening. However, in eq 20 we have counted all of the molecular encounters. According to McConnell the value of D_{diff} could be at most three times as great as the value given in the text.

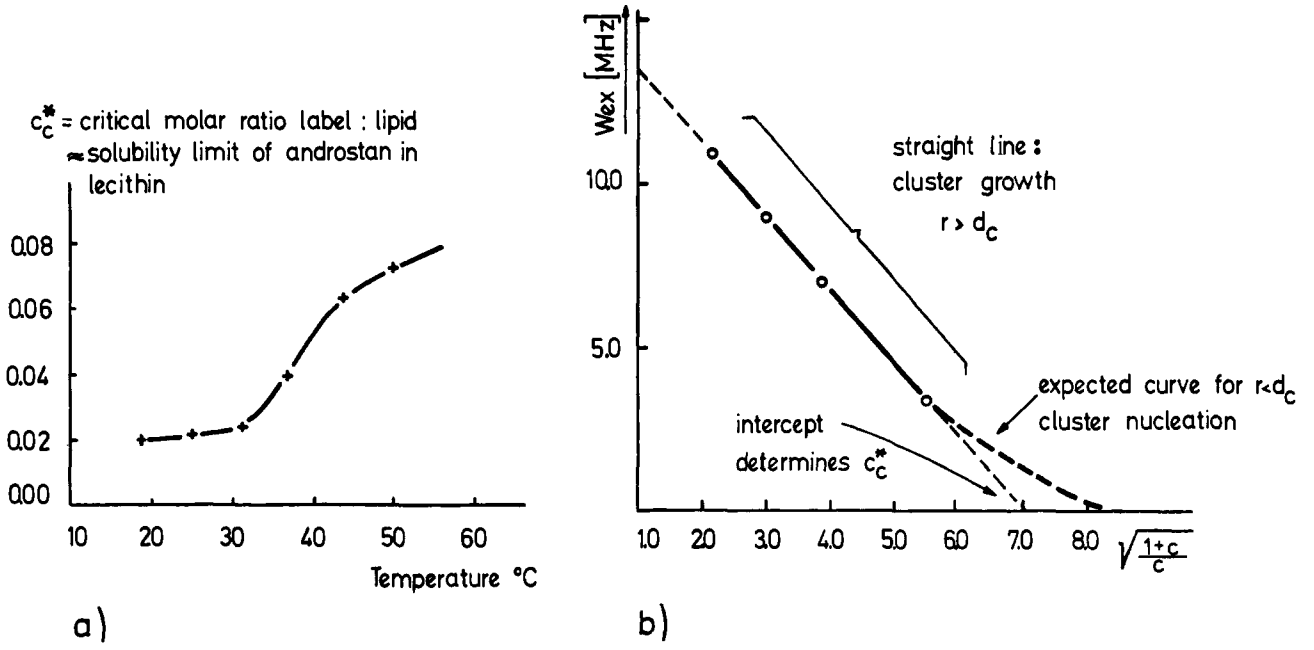

Figure 6. (a) Temperature dependence of the critical values c_c^* (c = molar ratio label:lipid) obtained from the curves in Figure 3. These values represent upper limits for the solubility of the androstane molecule (Figure 1) within dipalmitoyllecithin membranes. (b) Procedure for the determination of c_c^* values. According to the theory straight lines in the $W_{ex} \propto \sqrt{(1+c)/c}$ plot are expected for the growth phase of the steroid clusters. The c_c^* values are obtained as the intercepts with the abscissa of the $W_{ex} \propto \sqrt{(1+c)/c}$ tangents (*cf.* Figure 3). For small steroid concentrations, when $r \lesssim d_c$ (*cf.* Figure 7), deviations from straight lines are expected as indicated. The c_c^* values are not strictly identical with solubility limits, but they represent upper limits for the solubility.

drocarbon chains (*cf.* introduction to part I) and therefore should facilitate the diffusional motion of the steroid molecules. Summarizing we may say that the diffusional model describes correctly the situation above the phase transition ($T \gg T_t$) where $W_{ex} \propto c/(1+c)$ in accord with eq 23. The situation below T_t and the temperature dependence of W_{ex} in the range $T \lesssim T_t$ is, however, not in accord with this model.

3.3. Mosaic Model for $T \ll T_t$. It is characteristic for the situation below T_t that straight lines are obtained in a $W_{ex} \propto \sqrt{(1+c)/c}$ plot (Figure 3) and that these lines extrapolate to lower critical concentrations c_c^* characterized by $W_{ex} = 0$ when $c < c_c^*$. The values of c_c^* and the corresponding label distances d_c^* are given in Table II. The asterisk is used to indicate that these critical values are not necessarily identical with the above introduced values c_c and d_c. The existence of limiting concentrations c_c^* indicates that the steroid molecules cannot perform substantial translational motions. This rules out a diffusional model.

Two explanations for the critical values are conceivable. (1) For statistically distributed immobilized radicals, the critical values would be related to the sharp decrease of the exchange interaction with increasing radical distance d_{la} [$W_{ex} \approx$ constant ($\neq 0$) for $d < d_c$ and $W_{ex} \approx 0$ for $d > d_c$]. Therefore $W_{ex} = 0$ for $d_{la} > 2d_c$. However, the observed $W_{ex} \propto \sqrt{(1+c)/c}$ dependence is not compatible with a statistical distribution of the steroid molecules (*cf.* section 3.1) and the values of d_c calculated from the critical concentrations c_c^* are rather large ($d_c^* \approx 50$ Å). (2) The critical values c_c^* could be due to a limited solubility of the steroid molecules within the lipid matrix. This means that for $c < c_c^*$ the label molecules would be solubilized within the lipid matrix, and thus for $d_{la} > d_c$, $W_{ex} = 0$ as before. For $c \gtrsim c_c^*$ part of the steroid molecules would aggregate into small clusters within the lipid matrix (mosaic structure). Within these clusters the radicals are closely packed and strong exchange interaction becomes possible. This explanation is favored by the fact that the c_c^* values increase with increasing temperature, which can be understood as an increase in the solubility of the steroid molecules with increasing temperature. The dependence of the c_c^* values on temperature is shown in Figure 6a. For $T \ll T_t$ the c_c^* values are only weakly dependent on the temperature; however, a sharp increase by a factor of 3 occurs at the phase transition. Above T_t, c_c^* increases further with increasing temperature.

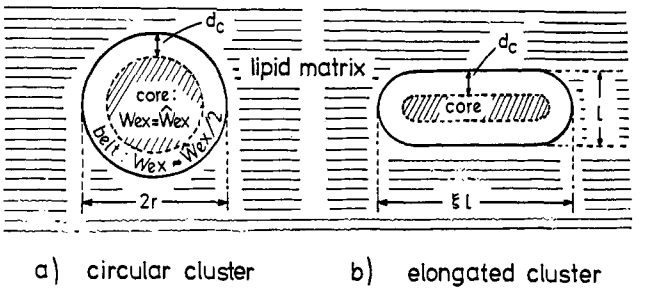

Figure 7. Schematic representation of closely packed steroid clusters embedded within the lipid matrix. (a) Circular cluster. The radius r of the cluster is assumed to be larger than the critical distance d_c for the onset of exchange interaction ($W_{ex} \approx 0$ for $d > d_c$). An inner core with radius $r_0 = r - d_c$ may be defined within which the radicals experience maximum exchange ($W_{ex} \equiv \hat{W}_{ex}$). In an outer belt of thickness d_c the exchange interaction of a given radical is smaller due to the reduced number of neighboring radicals. Here the average exchange interactions is approximately $W_{ex} = \hat{W}_{ex}/2$. (b) Elongated cluster with an axial ratio ξ.

An even stronger argument in favor of the mosaic structure is provided by the fact that the observed $W_{ex} \propto \sqrt{(1 + c)/c}$ dependence is a necessary corollary of this model. To show this we calculate the exchange frequency W_{ex} for circular clusters of closely packed steroid radicals (*cf.* Figure 7a). Our aim is to derive the dependence of W_{ex} on the cluster radius r. We consider at first clusters with a radius r larger than the critical distance d_c for the onset of exchange interaction ($d_c = 20$ Å). The cluster may be divided into an inner core of a radius $r_0 = r - d_c$ where the radicals experience maximum exchange interaction $\hat{W}_{ex}$. This core is surrounded by an outer belt of thickness d_c within which the exchange frequency is smaller because here a given radical has less radicals in its neighborhood. Within this zone the exchange frequency decreases from $W_{ex} = \hat{W}_{ex}$ at $r_0 = r - d_c$ to a value near zero at the cluster boundary. The density of radicals in the supporting lipid matrix is thus low that here $W_{ex} = 0$.

The average value of the exchange frequency in the belt can be written as

$$W_{ex}(\text{belt}) = \delta \cdot \hat{W}_{ex}$$

where $0 \leqslant \delta \leqslant 1$. Denoting with $\rho_{1a}{}^{cl}$ the radical density within the cluster the average exchange frequency W_{ex} within the cluster can be expressed as

$$W_{ex}\pi r^2 \rho_{1a}{}^{cl} = \underbrace{\pi(r - d_c)^2 \rho_{1a}{}^{cl} \hat{W}_{ex}}_{\text{contribution of the core}} + \underbrace{2\pi[(r - d_c)/2] d_c \rho_{1a}{}^{cl} \hat{W}_{ex} \cdot \delta}_{\text{contribution of the belt}} \quad (24)$$

For d_c small compared to r we obtain

$$W_{ex} = \hat{W}_{ex}[1 - 2(d_c/r)(1 - \delta)] \quad (25)$$

Taking approximately $\delta = {}^1/_2$ we find

$$W_{ex} = \hat{W}_{ex}[1 - d_c/r] \quad (26)$$

W_{ex} can be related to the molar ratio label:lipid, c, and the density n of clusters per cm^2 in the following way. The radical density ρ_{1a} may be written in the form

$$\rho_{1a} = nN = n\pi r^2 \rho_{1a}{}^{cl} \quad (27)$$

where $N = \pi r^2 \rho_{1a}{}^{cl}$ denotes the number of radicals per cluster. Identifying expression 27 with eq 3 leads to

$$r = (1/\sqrt{n}\sqrt{\pi})\sqrt{c/(1 + c)} \quad (28a)$$

Insertion into eq 26 yields

$$W_{ex} = \hat{W}_{ex} - \sqrt{\pi} d_c \sqrt{n} \sqrt{(1 + c)/c} \hat{W}_{ex} \quad (29)$$

This is the observed functional dependence between W_{ex} and c. We note that eq 29 is valid for the growth phase of (nonoverlapping) clusters with a radius r larger than d_c. More precisely the range of validity of eq 29 is $d_c \leqslant r < {}^1/_2(1/\sqrt{n} - d_c)$.

For the quantitative evaluation of the experimental results we identify the slope γ of the straight lines in Figure 3 with the derivative of expression eq 29

$$\gamma = \frac{dW_{ex}}{d\sqrt{(1 + c)/c}} = -\sqrt{\pi} d_c \sqrt{n} \hat{W}_{ex} \quad (30)$$

The numerical evaluation is given below.

To judge the validity of the derived equations we have varied the assumptions of the mosaic model in several respects. It is found that the $W_{ex} \propto \sqrt{(1 + c)/c}$ relation does not depend upon the exact shape of the clusters. However, the slope $dW_{ex}/d\sqrt{(1 + c)/c}$ is somewhat different for clusters of different shape.

Expression 28a is valid for $c > c_s$, where c_s is the solubility limit of the steroid molecules within the lipid material (no clusters for $c < c_s$). For low values of c we must consider that a certain amount of steroids molecules may be in "solution." Denoting $\rho_{1a}{}^{cl}$ = density of radicals in the clusters, $\rho_{1a}{}^{sol}$ = density of radicals in solution, and ρ_{1a} = total density of radicals, we can write

$$\rho_{1a} = \rho_{1a}{}^{cl} + \rho_{1a}{}^{sol}$$

and with eq 3

$$\rho_{1a} = \frac{1}{F}\frac{c}{(1 + c)}$$

$$\rho_{1a}{}^{sol} = \frac{1}{F}\frac{c_s}{(1 + c_s)}$$

Thus eq 27 is replaced by

$$\rho_{1a}{}^{cl} = \frac{1}{F}\left[\frac{c}{1 + c} - \frac{c_s}{1 + c_s}\right] = n\pi r^2/F$$

leading to

$$r = \frac{1}{\sqrt{n}\sqrt{\pi}}\sqrt{\frac{c}{1 + c} - \frac{c_s}{1 + c_s}} \quad (28b)$$

This indicates that eq 28 and 32 are valid only for $c/(1 + c) \gg c_s/(1 + c_s)$. The solubility limit c_s is between the critical values c_c extrapolated from Figure 3 and $c = 0.01$. For the latter concentration, clearly resolved triplet spectra were observed, indicating the absence of exchange interaction (*cf.* part I). Thus $c_c{}^* \geqslant c_s \gtrsim 0.01$.

Taking $c_s \approx 0.01$ it is easily checked that for $c = 0.035$, 0.075, 0.13, and 0.27 the values of $c/(1 + c)$ are by a factor 3.5–30 larger than $c_s/(1 + c_s)$. Thus in our experiments $c/(1 + c) \gg c_s/(1 + c_s)$, and therefore eq 28a and 32 can be used.

Since for $c = 0.01$ clearly resolved triplet spectra were observed, apparently the solubilized radicals do not contribute to the exchange interaction; thus the measured exchange interaction for $T \ll T_t$ is due to the aggregated radicals only.

The case of elongated clusters (*cf.* Figure 7b) can be treated in a similar way. For clusters with an axial ratio ξ large compared to one we find

$$W_{ex} = \hat{W}_{ex}[1 - d_c/l] \quad (31)$$

similar to eq 26. Further

$$l = \frac{1}{\sqrt{n}\sqrt{\xi}}\sqrt{\frac{c}{1 + c}} \quad (32)$$

Insertion into eq 31 yields

$$W_{ex} = \hat{W}_{ex} - d_c \sqrt{n} \sqrt{\xi} \sqrt{\frac{1 + c}{c}} \hat{W}_{ex} \quad (33)$$

Table III. Parameters of the Mosaic Structure (*cf.* Figures 7a and 8) with Circular Steroid Clusters Embedded within the Lipid Matrix ($T < T_t$)[a]

				(A)[b]			
				d_c = 15 Å		d_c = 25 Å	
T, °C	$\hat{W}_{ex}$, MHz[c]	$\lvert\gamma^c\rvert$	$\lvert\gamma\rvert/\sqrt{\pi}\hat{W}_{ex} = d_c\sqrt{n}$	n, l./cm²	$D = 1/\sqrt{n}$, Å	n, l./cm²	$D = 1/\sqrt{n}$, Å
19	13.4	2.10	0.088	3.36×10^{11}	170	1.22×10^{11}	285
31	11.5	2.09	0.103	4.75×10^{11}	145	1.68×10^{11}	245

		(B)[d]						
		d_c = 15 Å			d_c = 25 Å			
c	$\sqrt{c/(1+c)}$	r, Å	D, Å	N	r, Å	D, Å	N	r/d_c
0.27	0.461	44.0	170	152	74	285	430	2.96
0.13	0.34	32.5	170	83	55	285	237	2.1
0.075	0.265	25.5	170	51	40	285	125	1.7
0.035	0.185	17.8	170	25	28.5	285	64	1.2

[a] The experimental curves in Figure 3 yield the values for the maximum exchange frequency $\hat{W}_{ex}$ and the slopes γ. [b] (A) Evaluation of the experimental data according to the expression $\gamma = -\sqrt{\pi}d_c\sqrt{n}\hat{W}_{ex}$ (*cf.* eq 30) for two values of the critical cut-off distance d_c (d_c = 15 Å, d_c = 25 Å). n = cluster density per cm²; $D = 1/\sqrt{n}$ = average distance between the clusters. [c] From Figure 3. [d] (B) The radius r of the clusters and the number N of steroid molecules per cluster are listed for different values of the molar ratio label:lipid c at T = 19°. Evaluation according to the expressions $N = \pi r^2\rho_{1a}^{cl}$ and $r = (1/\sqrt{n}\sqrt{\pi})\sqrt{c/(1+c)}$.

and

$$\gamma = \frac{dW_{ex}}{d\sqrt{(1+c)/c}} = -\sqrt{\xi}d_c\sqrt{n}\hat{W}_{ex} \qquad (34)$$

This expression differs from eq 30 by the factor $\sqrt{\xi}/\sqrt{\pi}$. The absolute value of γ increases with $\sqrt{\xi}$; this is not unexpected because ξ determines the area ratio between the cluster core (maximum exchange interaction) and the cluster belt (reduced exchange interaction).

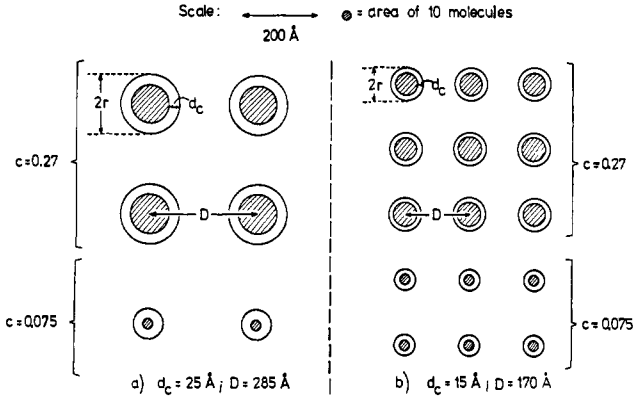

Figure 8. To-scale representation of steroid clusters embedded within the lipid matrix drawn for different values of the molar ratio label:lipid c and for two values of the critical cut-off distance d_c for the onset of exchange interaction ($W_{ex} = 0$ for $d > d_c$). The dimensions correspond to the values listed in Table III. Increasing label concentration results in a growth of the clusters at constant cluster distance D. A comparison between (a) and (b) shows the influence of the value of d_c on the cluster size and array. A similar figure can be drawn for the case of elongated clusters using the values given in Table V.

4. Evaluation of the Experiments

In order to calculate the parameters of the cluster model from our measurements, the value of the cut-off distance d_c must be known. Upper and lower limits of d_c can be established as follows. Sharp interaction-free triplet spectra are observed for $c \lesssim 0.017$. Thus d_c is certainly smaller than the corresponding average label distance d_{1a} = 58 Å, calculated from eq 5 with F = 48 Å². On the other side theoretical studies[10] show that the range of exchange interaction between two interacting radicals is about 15 Å. Thus a reasonable value of d_c is about 20 Å. To see how the choice of d_c affects the numerical results, we have evaluated the experiments for d_c = 15 Å and d_c = 25 Å.

4.1. Circular Clusters. Identification of expression 30 with the slopes γ in Figure 3 (*cf.* Table II) leads to

$$\gamma = -d_c\sqrt{n}\sqrt{\pi}\hat{W}_{ex} \qquad (35)$$

$\hat{W}_{ex}$ can be read from Figure 3 as the intercept of the straight lines with the ordinate at $c \to \infty$ (*cf.* Table II). The values of $d_c\sqrt{n}$, of n and $D = 1/\sqrt{n}$ (D = distance between clusters, *cf.* Figure 8), calculated for d_c = 15 Å and d_c = 25 Å are listed in Table III. The cluster radius r can be calculated using eq 28a and the number N of steroid molecules per cluster is obtained from

$$N = \pi r^2\rho_{1a}^{cl} \qquad (36)$$

where $\rho_{1a}^{cl} = 1/F$ and $F \approx 40$ Å² for the steroid molecules. The results are given in Table III(B).

We note that for all concentrations $c/d_c > 1$ which confirms the validity of our model. For a given value of d_c and a given temperature the cluster distance D is constant at all concentrations. For T = 19° the values of D are D = 170 Å for d_c = 15 Å, and D = 285 Å for d_c = 25 Å. The cluster density n increases somewhat with increasing temperature, for example, $n(31°) = 4.75 \times 10^{11}$ cm^{-2} and $n(19°) = 3.36 \times 10^{11}$ cm^{-2} for d_c = 15 Å. According to Table III(B) the size of the clusters depends on the label concentration. For d_c = 15 Å the cluster radius is r = 17.8 Å for c = 0.035 and r = 44 Å for c = 0.27. This corresponds to a number of steroid molecules per cluster of N = 25 and N = 152, respectively.

Figure 8 gives a to-scale representation of the distances and dimensions of the mosaic pattern for combinations of c = 0.27, c = 0.075 and d_c = 15 Å, d_c = 25 Å. This figure should be considered in conjunction with the radius r_V of our vesicles. For the limits r_V = 300 Å and r_V = 500 Å, the vesicles contain 35 and

Table IV. Number of Clusters per Spherical Lipid Monolayer Vesicle[a]

r_V = radius of vesicles, Å	Number of clusters per vesicle: d_c = 15 Å (D = 170 Å)	d_c = 25 Å (D = 285 Å)
300	35	11
500	100	36

[a] Calculated for two values of the vesicle radius: r_V = 300 Å and r_V = 500 Å and for two values of the cut-off distance d_c for the onset of exchange interaction (d_c = 15 Å and d_c = 25 Å). T = 19°.

The difference to the model of circular clusters is that for a chosen value of d_c the cluster density n and the distance D between the clusters depend upon the axial ratio ξ. Increasing values of ξ result in larger cluster distances and lower cluster densities.

The parameters of this model are given in Table V(B) for d_c = 15 Å, 25 Å and for ξ = 2 and 4. It is suggested that the axial ratio ξ is determined by the ratio of the lattice constants of the lipid matrix in the directions l_1 and l_2 (*cf.* Figure 5). This leads to $\xi \approx 2.3$.

Table V. Parameters of the Mosaic Structure with Elongated Steroid Clusters Having an Axial Ratio ξ (*cf.* Figure 7b)[a]

T, °C	$\hat{W}_{ex}$, MHz[c]	$\lvert\gamma^c\rvert$	$\lvert\gamma\rvert/\hat{W}_{ex} = d_c\sqrt{n}\sqrt{\xi}$ (Å)[b]	$\sqrt{n}\sqrt{\xi}$ (d_c = 15 Å)	$\sqrt{n}\sqrt{\xi}$ (d_c = 25 Å)
19	13.4	2.10	0.156	10.5×10^5	6.3×10^5
31	11.5	2.09	0.182	12.1×10^5	7.28×10^5

						(B)[d]					
						ξ = 2			ξ = 4		
c	$(1+c)/c$	$\hat{\xi} = [2(1+c)/c]\sqrt{c/(1+c)}$	l, Å	l/d_c		D, Å	N	n, l./cm²	D, Å	N	n, l./cm²
					d_c = 15 Å						
0.27	4.7	9.4	0.461	44	2.94	135	97	5.45×10^{11}	191	194	2.72×10^{11}
0.13	7.7	15.4	0.34	32	2.14	135	51.5	5.45×10^{11}	191	103	2.72×10^{11}
0.075	13	26	0.265	25.5	1.70	135	32.5	5.45×10^{11}	191	65	2.72×10^{11}
0.035	28	56	0.185	17.8	1.19	135	15.8	5.45×10^{11}	191	32	2.72×10^{11}
					d_c = 25 Å						
0.27	4.7	9.4	0.461	74	2.96	228	275	1.92×10^{11}	323	550	0.9×10^{11}
0.13	7.7	15.4	0.34	55	2.20	228	152	1.92×10^{11}	323	303	0.9×10^{11}
0.075	13	26	0.265	40	1.60	228	80	1.92×10^{11}	323	160	0.9×10^{11}
0.035	28	56	0.185	28.5	1.14	228	41	1.92×10^{11}	323	81	0.9×10^{11}

[a] The experimental curves in Figure 3 yield values for the maximum exchange frequency $\hat{W}_{ex}$ and the slope γ. These data are evaluated for d_c = 15 Å and d_c = 25 Å. [b] (A) Evaluation according to the theoretical result $\gamma = -d_c\sqrt{n}\sqrt{\xi}\hat{W}_{ex}$ (*cf.* eq 34), where n denotes the cluster density. [c] From Figure 3. [d] (B) Parameters characterizing the structure at T = 19° for different values of the molar ratio label: lipid c and for d_c = 15, 25 Å and ξ = 2, 4. Notations: l = thickness of clusters ($l = (1/\sqrt{\xi}\sqrt{n})\sqrt{c/(1+c)}$; $D = 1/\sqrt{n}$ = average distance between the clusters; N = number of steroid molecules per cluster ($N = l^2\xi/F$, where F = 40 Å²).

100 clusters assuming d_c = 15 Å; the corresponding values for d_c = 25 Å are 11 and 36, respectively (*cf.* Table IV).

4.2. Elongated Clusters. This model can be evaluated in much the same way as before. The theoretical expression for γ contains now as an additional parameter the axial ratio ξ (*cf.* Figure 7b). Identification of expression 34 with the measured slope γ yields

$$\gamma = -d_c\sqrt{n}\sqrt{\xi}\hat{W}_{ex} \tag{37}$$

The values of $\sqrt{n}\sqrt{\xi}$ are given in Table V(A) for d_c = 15 Å and d_c = 25 Å.

According to eq 32 the thickness of the clusters is

$$l = \sqrt{n}\sqrt{\xi}\sqrt{c/(1+c)}$$

l has the same numerical value as the radius r of the circular clusters. The expression for l may be rearranged to yield the density n of the clusters

$$n = c/(1+c)(1/l^2\xi) \tag{38}$$

The distance D between the clusters is

$$D = 1/\sqrt{n} = l\sqrt{\xi}\sqrt{(1+c)/c} \tag{39}$$

and the number N of radicals per cluster is

$$N = l^2\xi/F \tag{40}$$

where F = molecular area of steroid molecules ($F \approx 40$ Å²).

Two criteria may be applied to judge whether the grouping of the steroid molecules is better described by circular or elongated clusters. The calculated parameters of the two models should be compatible with the conditions

$$r \gg d_c, \text{ for circular clusters} \tag{41}$$

and

$$l < 2d_c, \text{ for elongated clusters} \tag{42}$$

For the lowest concentration, c = 0.035, these conditions are only weakly fulfilled. This has an obvious reason: at low concentrations the clusters are so small that a core with maximum exchange interaction does not exist. This case will be considered below (section 4.3). For higher concentrations both conditions are fulfilled and thus from conditions 41 and 42 a decision cannot be made between the two cluster shapes.

From the anisotropy of the lipid lattice (*cf.* Figure 5) it would, however, be anticipated that the growth rate of the clusters is different in the two directions l_1 and l_2. This would lead to elongated clusters. The model of elongated clusters is, of course, only valid as long as the clusters do not overlap. This leads to the condition

$$\xi l \leqslant D$$

or using eq 39

$$\xi \leqslant \hat{\xi} = (1+c)/c$$

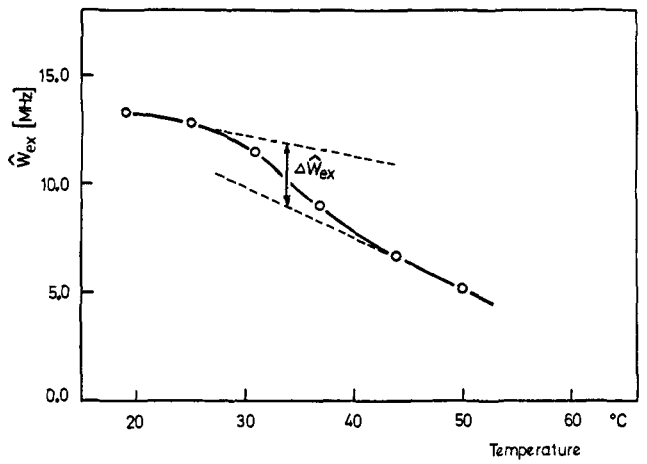

Figure 9. Temperature dependence of the maximum exchange frequency $\hat{W}_{ex}$ within the cores of the steroid clusters. The values of $\hat{W}_{ex}$ were determined from Figure 3 as the intercepts of the extrapolated curves with the ordinate at $c \rightarrow \infty$. The decrease of $\hat{W}_{ex}$ in the region of the lipid-phase transition corresponds to a lattice expansion of about 23% in very good agreement with X-ray data.[4,5] The slope $d\hat{W}_{ex}/dT$ determines the thermal expansion of the lipid matrix (see text).

The maximum values of the axial ratio $\hat{\xi}$ are given in Table V(B); they range between 10 and 60. Thus the proposed value $\xi \approx 2.3$ is well within the range of validity of this model. Thus there are arguments which favor elongated clusters over circular clusters. The general conclusions to be drawn from the cluster model are, however, not affected by this question.

4.3. Cluster Model for $r \lesssim d_c$ (Small Clusters). With decreasing steroid concentration the cluster radius decreases according to eq 28a and finally $r \lesssim d_c$. In this region eq 24 must be replaced by eq 15. For $d_o \approx 0$ this equation reads

$$W_{ex} = \pi A \rho_{1a}^{cl} r^2$$

where ρ_{1a}^{cl} denotes the density of steroid molecules within the clusters. For low concentrations r^2 is given by eq 28b and therefore

$$W_{ex} = \frac{A\rho_{1a}^{cl}}{n}\left[\frac{c}{1+c} - \frac{c_s}{1+c_s}\right] \qquad (43)$$

Thus for low label concentrations W_{ex} is expected to deviate from straight lines in the $W_{ex} \propto \sqrt{(1+c)/c}$ plot in the way indicated in Figure 6b. No experimental data are available for this range of concentration.

4.4. Temperature Dependence of $\hat{W}_{ex}$. Extrapolation of the curves in Figure 3 to $c \rightarrow \infty$ yields maximal values of the exchange frequency, $\hat{W}_{ex}$. $\hat{W}_{ex}$ represents the value of the exchange frequency within close-packed steroid clusters. Most probably the packing of the steroid molecules within the (relatively small) clusters is determined by the packing of the supporting lipid matrix. Therefore the temperature dependence of $\hat{W}_{ex}$ reflects the temperature dependence of the lattice constant of the lipid matrix.

This interpretation is supported by the following experimental evidence. Low angle X-ray diffraction studies[4,5] show that the molecular area of the lipid molecules increases by about $\Delta F/F \approx 20\%$ at the phase transition with increasing temperature. Thus from eq 17 it is expected that the phase transition produces a decrease in $\hat{W}_{ex}$ by $\Delta\hat{W}_{ex}/\hat{W}_{ex} \approx 20\%$. The value of $\Delta\hat{W}_{ex}/\hat{W}_{ex}$ determined from Figure 9 is $\Delta\hat{W}_{ex}/\hat{W}_{ex} \approx 23\%$. This suggests that the slope $d\hat{W}_{ex}/dT$ of the curve in Figure 9 reflects the temperature dependence of the lattice constant a of the lipid matrix. From Figure 9 we read

$$d\hat{W}_{ex}/dT = 10^5/(\text{sec °C}), \text{ for } T \ll T_t$$

and

$$d\hat{W}_{ex}/dT = 2.4 \times 10^5/(\text{sec °C}), \text{ for } T \gg T_t$$

Using eq 15 in the approximation $B = 1$ (or $d_o \approx 0$) we derive

$$d\hat{W}_{ex}/dT = -2\pi\frac{A}{\alpha^2 F^2}\frac{dF}{dT}$$

Substituting $A/\alpha^2 = \hat{W}_{ex}F/2\pi$ yields

$$d\hat{W}_{ex}/dT = -\hat{W}_{ex}/F\,(dF/dT)$$

Using eq 13 we obtain $d\hat{W}_{ex}/dT = -2\hat{W}_{ex}/a \cdot da/dT$.

$T \ll T_t$. According to Figure 9 $\hat{W}_{ex} \approx 14 \times 10^6$ Hz and $d\hat{W}_{ex}/dT = -10^5/(\text{sec °C})$. Taking $a = 4.19$ Å[5] we obtain for the temperature coefficient of the lattice constant the relation

$$da/dT \approx 0.02 \text{ Å/°C}$$

$T \gg T_t$. A similar consideration yields

$$da/dT \approx 0.07 \text{ Å/°C}$$

Thus the thermal expansion of the lipid lattice is by a factor of about 3 larger above the phase transition.

5. Discussion

The present work shows that the spin-label technique is a powerful method for the analysis of the organization of mixed membranes. The procedure applied in the present work involves three steps: (1) measurements of the esr line shape as a function of temperature and of the concentration of the labeled membrane component (*cf.* part I); (2) computer analysis of the esr spectra in order to determine the parameters of the magnetic interaction between the label molecules (*cf.* part II); (3) comparison of the experimental results with theoretical models for the organization of the mixed system.

The most striking result of our studies is the observation that the organization of the androstane–lecithin membranes depends critically upon the physical state of the lipid molecules. The two organization forms of our system present below and above the lipid phase transition are shown schematically in Figure 10.

Below T_t the solubility for steroid molecules in the lipid matrix is low, $c_s \lesssim c_c^* \approx 0.01$ (*cf.* Figure 6a). The steroid molecules can undergo tumbling motions within the lipid matrix with an average tumbling frequency of about 10^8 Hz; however, a substantial translational diffusion within the plane of the membrane is not possible. When the molar ratio steroid:lecithin exceeds a critical value $c_s \approx 0.03$ the steroid molecules start to aggregate into closely packed submicroscopic clusters. The size of the clusters increases with in-

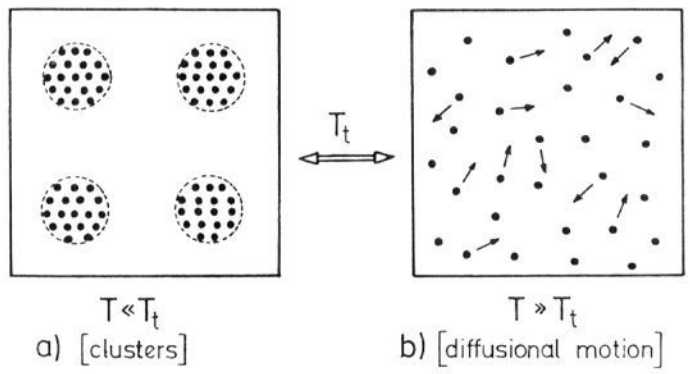

Figure 10. Molecular organization of steroid–lecithin membranes (a) below and (b) above the lipid-phase transition (schematically). (a) Below T_t the lipid matrix contains clusters of closely packed steroid molecules. The steroid molecules undergo tumbling motions but they cannot perform diffusional motion within the plane of the membrane. (b) Above T_t the steroid molecules are solubilized within the lipid matrix. The steroid molecules can undergo translational diffusion within the plane of the membrane. The thermal transition between the two states is reversible.

creasing label concentration whereas the density n of the clusters is independent of c. For $T = 19°$ n has a value of $3.36 \times 10^{11}/cm^2$. Most likely the clusters are elongated and have an axial ratio of about $\xi \approx 2.5$.

Above T_t the solubility for steroid molecules is considerably larger (*cf.* Figure 6a). Up to fairly high concentrations ($c = 0.1$) the system consists of a homogeneous mixture of steroid and lecithin molecules. In addition to a very fast tumbling motion with a frequency of 3×10^8 Hz the steroid molecules undergo translational diffusion within the plane of the membrane. The diffusion coefficient ($D_{diff} \approx 10^{-8}$ cm^2/sec) is three orders of magnitude smaller than the typical values for the self-diffusion in liquids. This difference is due to the fact that in our case the diffusing molecules are rather large and that the membrane exhibits considerable order. The hopping frequency ν for the steroid molecules within the lipid membrane is $\nu \approx 3 \times 10^6$/sec. Thus the average travel distance in 1 sec is about 10,000 Å, corresponding to the length of about 1400 lattice distances.

In biological membranes diffusional processes within the plane of the membranes are probably important in the formation of specific groupings (functional complexes) of different molecules. We conclude from our results that this process is possible only when the membrane lipids are in a state above T_t.

The thermal transition between the two structures in Figure 10 is reversible. Upon heating the system above T_t the clusters dissolve and the steroid molecules become free to diffuse around within the plane of the membrane. Upon cooling, reaggregation takes place. This aggregation produces the sharp increase in the exchange frequency W_{ex} when the temperature falls below T_t.

The change in the organization of the mixed system at T_t may be considered as a result of the increase in "fluidity" of the lipid hydrocarbon chains at T_t. It will be recalled that low angle X-ray investigations[4,5] show that for $T < T_t$ the lipid molecules are in a quasi-crystalline state in which the hydrocarbon chains may be considered approximately as rigid rods. As demonstrated in Figure 11a the steroid molecules cannot be accommodated very well within such a structure. In the environment of the steroid molecules pockets of free volume are created corresponding to a loss in interaction between the hydrocarbon chains. Thus by aggregation of the steroid molecules the free energy of the system can be lowered.

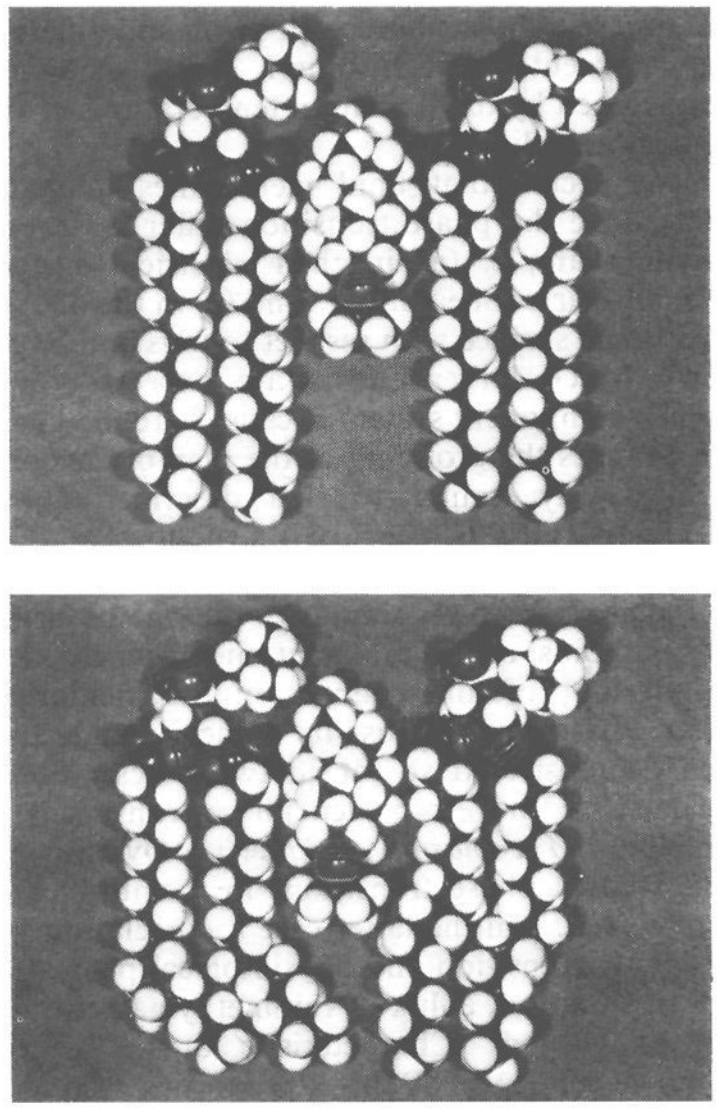

Figure 11. Pauling–Corey–Koltun model showing steroid molecule sandwiched between two lipid molecules. (a) The lipid hydrocarbon chains are considered as rigid rods: situation below the lipid-phase transition. (b) Above the lipid-phase transition the hydrocarbon chains can form rotational isomers (kinks); the chains are flexible and can accommodate the steroid nucleus much better. This figure explains why clusters are formed for $T < T_t$ and why the steroid molecules are solubilized much better above the phase transition.

Above T_t the hydrocarbon chains are more "fluid." In a previous paper[11] an attempt has been made to describe this state in terms of the presence of rotational isomers ("kinks") of the hydrocarbon chains. Kinks are mobile structural defects which can move along the hydrocarbon chains with a diffusional coefficient $D_{diff} \approx 10^{-5}$ cm^2/sec. According to dilatometric and X-ray measurements the kink concentration increases with increasing temperature by one order of magnitude at the phase transition. The higher kink concentration at $T > T_t$ (about one kink per hydrocarbon chain) produces a high degree of static and dynamic disorder in the hydrocarbon chains. This state can be described in terms of a "flexing" and "twisting" of the chains. As demonstrated in Figure 11b steroid molecules can be much better accommodated by kinked hydrocarbon chains. This is the reason for the higher solubility of steroid molecules in the lipid matrix above T_t.

Our results can be discussed in terms of the structure and function of biological membranes and the action of steroid molecules on membrane properties.

1. The demonstration of a mosaic structure in the androstane–lecithin system suggests that biological membranes containing several components may well exhibit rather complicated molecular groupings with

regions of different molecular composition and different properties adjacent to each other. Such groupings could be governed by the transition temperatures of the different membrane lipids.

2. It is expected that lipid membranes in states below and above the phase transition differ in several respects, for example, (a) in their electrical surface charge, (b) in their permeability,[19] and (c) in the affinity of the membrane surface with respect to ions and larger molecules.[8] Much larger effects are expected for a two- or multi-component system because here the phase transition changes the grouping of the membrane components in a way similar to that described above (mosaic pattern for $T \ll T_t$, mixed structure for $T \gg T_t$).

Thus, if phase transitions similar to the one observed with phospholipids occur in intact membranes, they would result in profound changes in the membrane properties. Phase transitions in intact membranes have been demonstrated so far in two cases. Steim and colleagues[20-22] have reported phase transitions in membranes of *Mycoplasma Laidlawii*. Overath, *et al.*,[23] have studied phase transitions in membranes of mutants of *E. coli*. In the latter case a correlation between the phase transition and physiological properties of the cell (respiration, efflux of thiomethylgalactoside) has been established. Characteristic breaks in the temperature dependence of these properties were observed at defined temperatures. These temperatures are affected by the structure of the lipid molecules in the same way as with synthetic lipids. In collaboration with Dr. P. Overath we have applied our spectroscopic methods to both the isolated lipids and the intact membranes of such *E. coli* mutants. The main lipid components (cephalins) show phase transitions in the same temperature range in which abrupt changes of the physiological properties were observed. With the intact membranes the phase transitions could be detected optically using the hydrophobic fluorescent probe *N*-phenyl-1-naphthylamine.[24] Using the androstane spin label, we obtained esr spectra almost identical with the spectra in Figure 7 (part I). The temperature and concentration dependence of the esr spectra were studied systematically with a fatty acid nitroxide label incorporated into the intact membranes. In all cases we observed sharp changes in the order parameter S at temperatures where breaks in the physiological properties occurred (S is defined according to eq 14 in ref 44, part I). In complete analogy to our findings with the dipalmitoyllecithin system the state above T_t is characterized by a rapid lateral diffusion within the plane of the membrane. However, in the intact membranes (containing lipids with unsaturated hydrocarbon chains) the diffusion is three times faster. A detailed account of this work is in preparation.

3. Of course, thermally induced phase transitions are not expected to play a role in those living systems, which are at a constant temperature. There is, however, good evidence that the crystalline–liquid crystalline phase transition can be triggered also by other parameters, for example, by changes in the ionic environment, the pH, the transmembrane potential, or by the attachment of certain ligands to the membrane surface[25].

4. Concerning the action of steroid molecules on the membrane properties, it is conceivable that steroid molecules or clusters of steroid molecules provide patterns of groups to which proteins or other molecules could become attached specifically. This possibility has been suggested by Willmer.[26] Recent experiments[27,28] have shown that steroids are important for the interaction of ribosomes with endoplasmic membranes. Assuming that clusters of steroid molecules provide specific binding patterns for proteins, this would imply that the phase transition ($T < T_t \rightarrow T > T_t$), resulting in a disappearance of the clusters, would trigger the release of proteins from the membrane. This in turn would affect the metabolism of the cell.

Due to the large diversity in the chemical structure of the various steroid molecules it is hardly possible to proceed by analogy from the androstane–lecithin system to other steroid–lecithin systems. Cholesterol, which has a hydrocarbon tail in the 17 position, is known to be much better soluble within a lipid matrix than a "naked" steroid nucleus. The work by Demel, *et al.*,[29] shows that minor differences (*e.g.*, cholesterol → epicholesterol) have remarkable effects on the incorporation of sterols into lipid monolayers.

Clearly, more experimental work is necessary before general statements can be made as to the factors determining the organization of mixed steroid–lecithin systems. From the present work it is clear that measurements of the magnetic interaction between spin-labeled steroids by the esr technique provide a powerful method to investigate the organization of such mixed steroid–lecithin systems.

Acknowledgment. We are greatly indebted to Dr. H. M. McConnell for his expert criticism of our work. We are grateful to Dr. D. Haynes for discussions and for reading the manuscript. It is a pleasure to thank Dr. R. A. Demel and coworkers for making available their results prior to publication. The careful writing of the manuscript by Miss G. Klump is gratefully acknowledged.

(19) H. Träuble, *J. Membrane Biol.*, **4**, 193 (1971).
(20) J. M. Steim, M. E. Tourtellotte, J. C. Reinert, R. N. McElhaney, and R. L. Rader, *Proc. Nat. Acad. Sci. U. S.*, **63**, 104 (1969).
(21) J. M. Steim, *Advan. Chem. Ser.*, No. **84**, 281 (1968).
(22) J. C. Reinert and J. M. Steim, *Science*, **168**, 1580 (1970).
(23) P. Overath, H. U. Schairer, and W. Stoffel, *Proc. Nat. Acad. Sci. U. S.*, **67**, 606 (1970).
(24) H. Träuble and P. Overath, submitted for publication.
(25) H. Träuble, Symposium on Passive Permeability of Cell Membranes, Rotterdam, 1971; "Biomembranes," L. A. Manson, Ed., Plenum Press, New York and London, in press.
(26) E. N. Willmer, *Biol. Rev.*, **36**, 368 (1961).
(27) C. H. Sunshine, D. J. Williams, and B. R. Rabin, *Nature (London), New Biol.*, **230**, 133 (1971).
(28) C. A. Blyth, R. B. Freedman, and B. R. Rabin, *ibid.*, **230**, 137 (1971).
(29) R. A. Demel, K. R. Bruckdorfer, and L. L. M. van Deenen, *Biochem. Biophys. Acta*, **255**, 311, 324 (1972).